Author Manuscript

Title: Multi-electron Oxidation of Ce(III) Complexes Facilitated by Redox-Active Ligands

Authors: D. M. Ramitha Y. P. Rupasinghe; Lauren Marie Lopez; Andrew Thomas Poore; Makayla Baxter; Andrew W. Mitchell; Matthias Zeller; Shiliang Tian; Suzanne C. Bart, Ph.D.

To be cited as: 10.1002/ejic.202300761

Link to VoR: https://doi.org/10.1002/ejic.202300761

WILEY VCH

RESEARCH ARTICLE

Multi-electron Oxidation of Ce(III) Complexes Facilitated by Redox-Active Ligands

D. M. Ramitha Y. P. Rupasinghe, Lauren M. Lopez, Andrew T. Poore, Makayla R. Baxter, Nathan J. Lin, Andrew W. Mitchell, Matthias Zeller, Shiliang Tian and Suzanne C. Bart*[a]

[a] D.M.R.Y.P. Rupasinghe, L.M. Lopez, A.T. Poore, M.R. Baxter, N.J. Lin, A.W. Mitchell, Dr. M. Zeller, Prof. S. Tian, Prof. S.C. Bart
H.C. Brown Department of Chemistry
Purdue University
West Lafayette, Indiana 47907
E-mail: sbart@purdue.edu

Supporting information for this article is given via a link at the end of the document.

Abstract: A family of cerium complexes featuring a redox-active ligand in different oxidation states has been synthesized, including the the iminosemiquinone (isq)$^{1-}$ compound, Ce(^{dipp}isq)$_3$ (**1-Ceisq**), and the amidophenolate (ap)$^{2-}$ species Ce^{III}(^{dipp}ap)$_3$K$_3$ (**2-Ceap**), [Ce^{III}(^{dipp}ap)$_3$K][K(18-c-6)]$_2$ (**2-Ceap 18c6**), and [Ce^{III}(^{dipp}ap)$_3$K][K(15-c-5)$_2$]$_2$ (**2-Ceap 15c5**). Treating the latter species with dioxygen furnishes the cerium(IV) derivatives, [Ce^{IV}(^{dipp}ap)$_3$][K(15-c-5)$_2$]$_2$ (**3-Ceap 15c5**) and [Ce^{IV}(^{dipp}ap)$_3$][K(crypt)]$_2$ (**3-Ceap crypt**). Similarly, addition of hexamethyldisiloxane produces an interesting bis(amidophenolate) species, [(Me$_3$SiO)$_2$Ce^{IV}(^{dipp}ap)$_2$][K(15-c-5)$_2$]$_2$ (**4-CeOSiMe$_3$**). Full spectroscopic and structural characterization of each derivative was performed to establish the oxidation states of both the ligands and the cerium ions.

Introduction

The elements in the lanthanide series are known for their thermodynamically preferred +3 oxidation states; however, several outliers have energetically low-lying accessible oxidation states, giving them the ability to engage in redox chemistry.[1] One such example is cerium, which has an accessible III/IV redox couple that creates divergent chemistry for this lanthanide among its neighbors.[2, 3] This one-electron metal based redox couple can facilitate electron movement, but in the majority of instances it is limited to one electron steps.[3] A rare contradiction to this was recently published by Huang and co-workers, who reported that the cerium(II) derivative, [K(crypt)][(^{Ad}TPBN$_3$)Ce(II)] (H$_3$(^{Ad}TPBN$_3$) = 1,3,5-tris[2-(1-adamantyl)aminophenyl]benzene), undergoes two electron oxidation to generate a family of cerium(IV) complexes with multiply bonded terminal ligands.[4]

The rarity of the metal-based two electron redox couple for cerium demonstrates the need for further expanding the redox chemistry of cerium-based complexes. In the cases of metals where redox couples are not possible or energetically accessible, it has been established that redox-active ligands can facilitate such chemistry using their low-lying π^* orbitals.[5-7] For example, J. Arnold has demonstrated that storing two electrons in a bipyridine ligand facilitates reductive elimination at a thorium(IV) centre.[8] In the lanthanide row, Fedushkin and co-workers have presented extensive work on redox-active ligands supporting lanthanides,[9-12] such as the recent case of rare earth-dpp-Bian compounds (RE = Yb, Tm, or Dy) (dpp-Bian = 1,2-bis[(2,6-diisopropylphenyl)-imino]acenaphthene).[13] Mazzanti and co-workers have recently reported an exciting example where a cerium derivative supported by the LO$_3$ ligand framework (LO$_3$ = 1,3,5-(2-OSi(OtBu)$_2$C$_6$H$_4$)$_3$C$_6$H$_3$) has been isolated and characterized in four different redox states.[14] In this example, the central arene is redox active, storing electrons in delta bonds and facilitating this rich redox chemistry.

Our laboratories have had success with the iminoquinone/amidophenolate family of ligands, which can exist as the iminoquinone (iq), iminosemiquinone (isq), or amidophenolate (ap) forms, with respective oxidation states of 0, -1, and -2. Their bidentate nature is especially attractive as more than one ligand could surround the central metal ion, creating an opportunity for multiple electron storage.[15] One example shows the synthesis of a rare, paramagnetic thorium oxo, [O=Th(^{dipp}isq)$_2$(^{dipp}ap)[K(15-c-5)$_2$], from [Th(^{dipp}ap)$_3$][K(15-c-5)$_2$]$_2$ (isq = 4,6-di-*tert*-butyl-2-(R)-imino-semiquinone; ap = 4,6-di-*tert*-butyl-2-(R)-amidophenolate), which involved the oxidation of two amidophenolate ligands to iminosemiquinones.[16]

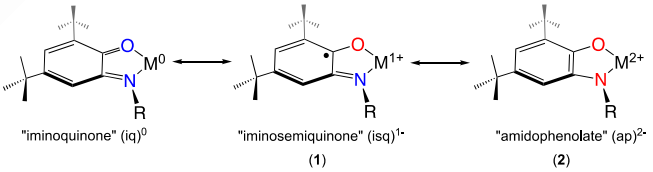

Figure 1: Redox chemistry for the iminoquinone/amidophenolate family of ligands. Blue atoms denote dative (neutral) bonding and red atoms denote anionic bonding.

Our group, along with Schelter and co-workers, recently reported the synthesis of Ce^{III}(^{dipp}ap)$_3$K$_3$ (**2-Ceap**), generated from reduction of CeCl$_3$ in the presence of iminoquinone ligand.[17] This species is paramagnetic due to the Ce^{III}, 4f^1 centre. Structural data were reported and shows that the potassium ions are situated within the tris(ligand) framework. While this compound is quite interesting, we hypothesized that reactivity would be enhanced if the countercations were removed from the coordination sphere. Herein, we report the synthesis and characterization of multiple species where potassium countercations are sequestered by chelating ligands. Our findings support that reactivity is enhanced with an open coordination sphere. Characterization of these species and their reaction products by ^{1}H NMR spectroscopy, X-ray crystallography,

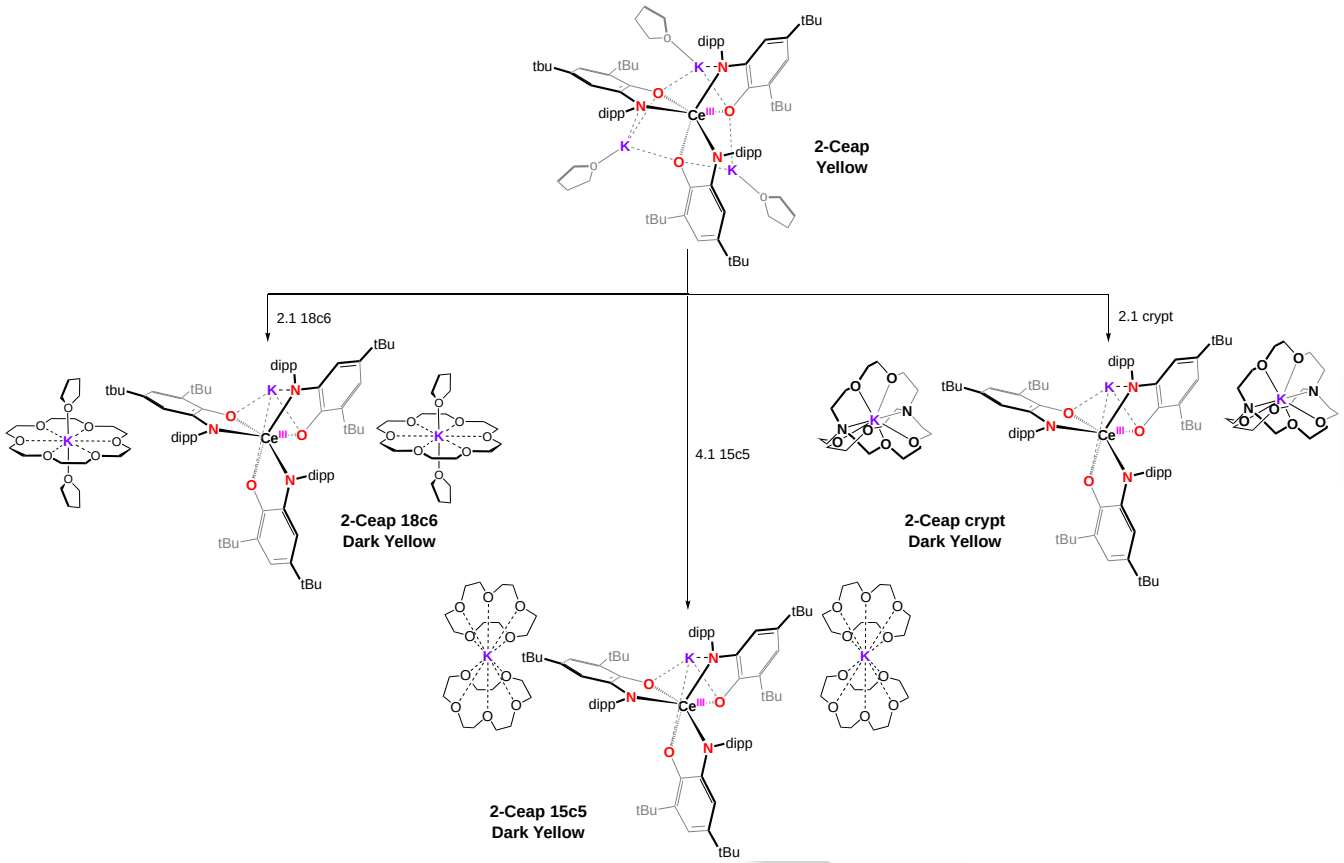

Scheme 1: Synthesis of **2-Ceap 18c6**, **2-Ceap 15c5**, and **2-Ceap crypt.**

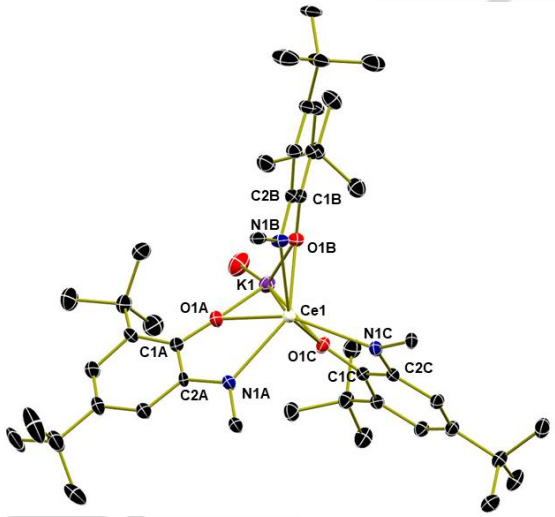

Figure 2: Molecular structure of **2-Ceap 15c5** shown with 30% probability ellipsoids. Hydrogen atoms, sequestered potassium ions with crowns, dipp groups, the carbons on the THF coordinated to the K1 atom and co-crystallized solvent molecules have been omitted for clarity.

electronic absorption spectroscopy, and electron paramagnetic resonance spectroscopy are reported herein.

Results and Discussion

Studies commenced to elucidate the molecular structures of **2-Ceap** when potassium countercations were sequestered from the reduced amidophenolate ligands. When a THF solution of 3.1 equivalents of 18-c-6 was added to a THF solution of **2-Ceap**, $[Ce^{III}(^{dipp}ap)_3K][K(18\text{-}c\text{-}6)]_2$ (**2-Ceap 18c6**) was isolated after workup (Scheme 1). The ^{1}H NMR spectrum revealed a large crown peak rendering the ligand resonances non-integrable and difficult to assign clearly (Figure S3). Several paramagnetic resonances were observed supporting a Ce(III), $4f^1$ ion, which would be expected given the closed shell ligands. Crystals of **2-Ceap 18c6** were grown from THF: Pentane (1:1) at room temperature and measured using X-ray diffraction; refinement of the data revealed a molecular structure with only two of the three potassium ions sequestered. This crystal structure was not of reasonable quality to obtain meaningful bond metrics, however.

Due to the poor quality of this data, 15-c-5 was also used to attempt potassium ion sequestration. A THF solution of 6.1 equivalents of 15-c-5 was added to a THF solution of **2-Ceap,** and $[Ce^{III}(^{dipp}ap)_3K][K(15\text{-}c\text{-}5)_2]_2$ (**2-Ceap 15c5**) was isolated after workup (Scheme 1). Similar to **2-Ceap 18c6**, the ^{1}H NMR spectrum of **2-Ceap 15c5** revealed a large crown singlet, rendering the other resonances difficult to definitively assign (Figure S4). The ^{1}H NMR spectrum again showed paramagnetic resonances similar to **2-Ceap 18c6**, supporting a $4f^1$ configuration for cerium. X-ray diffraction of single crystals grown from a THF:pentane (1:1) solution at -35°C revealed a crystal structure similar to **2-Ceap 18c6** with only two of the three potassium ions sequestered (Figures 2 and 3). In the case of **2-Ceap 15c5,** the cerium ion is six-coordinate, with a distorted octahedral geometry.

The C-O and C-N bond lengths of **2-Ceap 18c6** were similar to those of the parent **2-Ceap** at 1.336(3) – 1.387(3) Å and 1.387(3) – 1.430(18) Å, respectively, and consistent with the single bond nature of the amidophenolate ligand to the cerium. The Ce-O bond lengths are even shorter than for **2-Ceap (**2.3918(16) – 2.4082(17) Å) while the Ce-N bond lengths are longer (2.5142(19) – 2.5227(17) Å); both the Ce-O and Ce-N bond lengths are consistent with anionic single bonds.

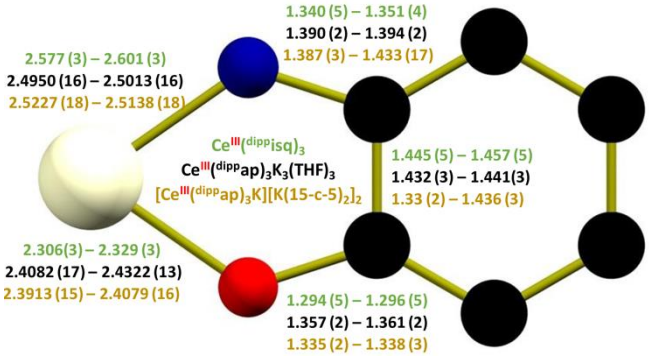

Figure 3. Bond distance comparison (Å) for **1-Ceisq (green)**, **2-Ceap (black)** and **2-Ceap 15c5 (gold)**. Carbon atoms shown in black, nitrogen in blue, oxygen in red, and cerium in white.

Given that not all the potassium ions were sequestered using the crowns, cryptand was also used. Potassium binding by [2.2.2]-cryptand is stronger in comparison to 18-c-6 and 15-c-5, with cryptand being 33,000 and 14.8 million times stronger in binding potassium compared to 18-c-6 and 15-c-5, respectively, in anhydrous methanol (based on stability constants, K_s).[18] Hence, a THF solution of 3.1 equivalents of cryptand was added to a THF solution of **2-Ceap**. After workup, $[Ce^{III}(^{dipp}ap)_3K][K(crypt)]_2$ (**2-Ceap crypt**) was isolated. Similar to **2-Ceap 15c5** and **2-Ceap 18c6**, **2-Ceap crypt** showed a paramagnetic ^{1}H NMR spectrum with large cryptand resonances rendering ligand resonances non-integrable and difficult to assign (Figure S5). Despite multiple attempts, a single crystal could not be isolated for **2-Ceap crypt**. However, given the similar ^{1}H NMR spectroscopic data, it was hypothesized that only two of the potassium ions were sequestered. The syntheses of **2-Ceap 15c5, 2-Ceap 18c6**, and **2-Ceap crypt** were done rationally with the appropriate equivalents of crown/crypt to furnish the final compounds in good yields (Scheme 1).

Cyclic voltammetry (CV) was used to elucidate oxidation potentials and oxidation state stability dependence on the sequestration of potassium ions. Voltammograms of **2-Ceap** were collected in THF (0.1 M NBu_4PF_6) (Figures S13, S14). The Ce(IV/III) couple was assigned as the large redox event at $E_{1/2}$ = $(E_{p,a} + E_{p,c})/2$ = -0.72 + -1.02)/2 = -0.87 V (± 50 mV) vs. $Fc^{+/0}$. Upon potassium sequestration, the electrochemical behavior of **2-Ceap 15c5** slightly changes (Figures 4, S15). Compound **2-Ceap 15c5** has the Ce(IV/III) couple at $E_{1/2}$ = -0.68 V, a potential shift of ca. 0.19 V positive from **2-Ceap**, indicating a stabilization of Ce(III) due to sequestration of potassium.

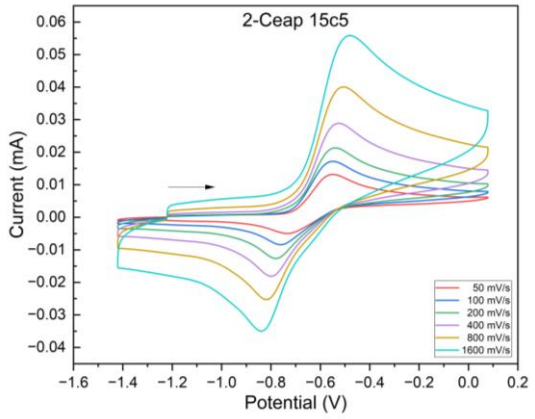

Figure 4. Cyclic voltammogram of **2-Ceap 15c5** collected in THF (0.1 M NBu_4PF_6) at ambient temperature; $E_{1/2}$ = -0.68 V vs. $Fc^{+/0}$.

Although the third potassium ion could not be removed from the inner coordination sphere with either the crown ethers or cryptands, reactivity of **2-Ceap 15c5, 2-Ceap 18c6**, and **2-Ceap crypt** was explored to understand their multi-electron reactivity. This family of compounds has an interesting electronic structure in that all ligands are highly reduced, and the cerium(III) still has one 4f electron ($4f^1$). Oxidation of these derivatives was attempted to determine whether the ligand or the cerium would be oxidized first. Addition of 1.5 equivalents of elemental iodine to **2-Ceap,** where the potassium ions are intercalated, resulted in oxidation of each of the amidophenolate ligands to the iminosemiquinone, forming **1-Ceisq** (Scheme 2). This oxidation reaction is similar to oxidation described with $Th(^{dipp}ap)_3K_2(THF)_2$ to form $Thisq_3I$.[15] The ^{1}H NMR spectrum of **1-Ceisq** was similar to the KC_8 synthesis route using $CeCl_3$ as the starting material with resonances for free ligand still present.

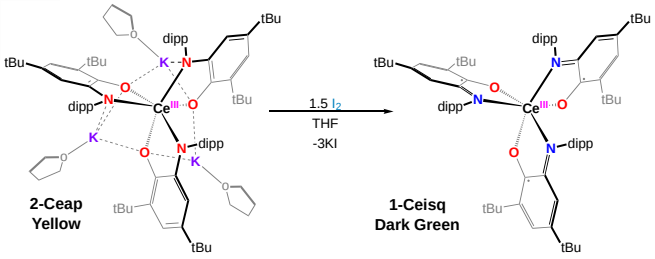

Scheme 2: Synthesis of **1-Ceisq** via oxidation of **2-Ceap.**

Several single crystals of **1-Ceisq** were grown from slow evaporation of hexanes (Figures 3 and 5). Analysis and refinement of the data shows a six coordinate cerium ion with a distorted octahedral geometry, lacking any counterions as this species is neutral. The C-O and C=N bond lengths are similar to those of previously published $Th(^{dipp}isq)_3Cl$, indicating single and double bond character respectively;[15] the C-O bond length of $Th(^{dipp}isq)_3Cl$ is 1.306(5) Å while for **1-Ceisq**, it is 1.294(5) – 1.296(5) Å. The C=N bond for $Th(^{dipp}isq)_3Cl$ is 1.342(5) Å as compared to 1.340(5) – 1.351(4) Å for [15][14][obs]. Ce-O single bonds average at about 2.45 Å and the Ce-O bond for **1-Ceisq** is less than that at 2.306(3) - 2.329(3) Å, indicating an anionic Ce-O [19, 20][17, 18][obs]. Ce-N bond of Ce-N=C complexes average at around 2.48 Å and the Ce-N bond for **1-Ceisq** is significantly longer than

that at 2.577(3) – 2.601(3) Å indicating a dative Ce-N [21, 22][19, 20][OB]. From these crystallographic data, it can be inferred that there are three iminosemiquinone ligands around the cerium for **1-Ceisq** similar to the published Th(^{dipp}isq)$_3$Cl complex. Thus, one electron oxidation of the amidophenolate has occurred three times to generate **1-Ceisq.**

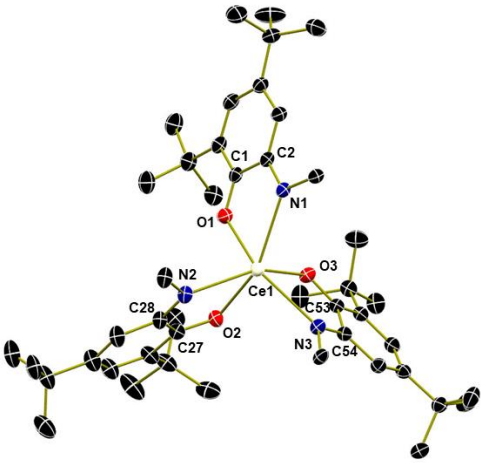

Figure 5: Molecular structure of **1-Ceisq** shown with 30% probability ellipsoids. Hydrogen atoms, dipp groups, and cocrystallized solvent molecules are omitted for clarity.

Further characterization of both **2-Ceap 15c5** and **1-Ceisq** was obtained using electronic absorption spectroscopy. Spectra for each were recorded in THF at 25 °C in the visible and NIR regions. For **2-Ceap 15c5**, smooth transitions are seen in the visible region, from 400-800 nm, with an absorption at 456 nm (ε = 366 M^{-1} cm^{-1}), which is likely responsible for the dark yellow color (Figure S10). In contrast, **1-Ceisq** has a strong absorption in the red at 766 nm (ε = 331 M^{-1} cm^{-1}), due to the ligand pi-to-pi* transition, giving this compound it's dark green appearance. In the NIR region, both **2-Ceap 15c5** and **1-Ceisq** show an absorption at 1384 nm with low molar absorptivities (ε = 20-40 M^{-1} cm^{-1}) assignable to the *f-f* transitions for the Ce(III), f^1 ion (Figure S11).

X-band electron paramagnetic resonance (EPR) was employed to investigate the spin localization and determine the ground state of **2-Ceap 15c5** and **1-Ceisq**, particularly in light of the redox non-innocent behavior exhibited by the amidophenolate ligands. Cerium(III), with its $4f^1$ electron configuration, typically shows significant deviations from the expected g-value (g_e = 2.0023) in an S = ½ system, primarily due to spin-orbital coupling effect.[23] Notably, the EPR spectrum of **2-Ceap 15C5** at 6 K showed an EPR signal around g ~ 2.5 (Fig. 5), aligning with previously reported characteristics of Ce(III) species.[2, 14] This spectrum is absent at room temperature, attributed to rapid spin-lattice relaxation. This observation suggests that the unpaired electron is predominantly localized at cerium, rather than as a ligand-based radical.

In previous EPR work with iminosemiquinone ligands, we established there is no apparent coupling between the two iminosemiquinone ligand-centered radicals in [O=Th(^{dipp}isq)$_3$][K(15-c-5)$_2$].[15] These ligands function as two independent S = ½ radicals, and their signals are detectable at room temperature using EPR spectroscopy. Surprisingly, for **1-Ceisq,** the room temperature EPR spectrum showed no signal typical for organic radicals (Fig. 5), suggesting that the three spins on the ligands are likely coupled with the paramagnetic Ce(III) center.

To further explore this, we conducted low temperature EPR measurements at 6 K on **1-Ceisq**. This showed a signal at g = 2, confirming the presence of an iminosemiquinone radical (Fig. 6). However, the **1-Ceisq** EPR spectrum also displayed a broad peak at g ~ 2.9, which is notably higher than that observed for **2-Ceap 15c5** (g ~ 2.5). This shift in the Ce(III) g-values, coupled with the attenuated iminosemiquinone signal at room temperature, suggests spin-spin interactions between the $4f^1$ electron and the iminosemiquinone radicals. Similar EPR characteristics have been observed in a reduced Ce(III) complex featuring a tripodal tris(di-*tert*-butoxylsilanol) arene ligand, where the reduction occurs at the ligand rather than at the Ce(III) center.[14]

More oxidation chemistry was explored by treating THF solutions of both **2-Ceap 15c5** and **2-Ceap crypt,** where 2 potassium ions are sequestered, in Schlenk flasks with 0.5 equivalents of dioxygen measured using a calibrated gas bulb (Scheme 3). Upon exposure to dioxygen, the amidophenolate compounds turned dark green, which can sometimes indicate oxidation of amidophenolate ligands to iminosemiquinone ligands. However, upon workup and characterization by X-ray crystallography, it was determined that oxidation occurred at the cerium rather than the amidophenolate ligands, furnishing [Ce^{IV}(^{dipp}ap)$_3$][K(15-c-5)$_2$]$_2$ (**3-Ceap 15c5**) and [Ce^{IV}(^{dipp}ap)$_3$]-[K(crypt)]$_2$ (**3-Ceap crypt**), respectively. It is hypothesized that the non-sequestered potassium ion could have combined with dioxygen, producing potassium oxides. This is in contrast to **1-Ceisq,** where ligand oxidation is noted. In this case, two of the potassium ions are outer sphere, which creates a more sterically accessible cerium centre, possibly facilitating metal oxidation.

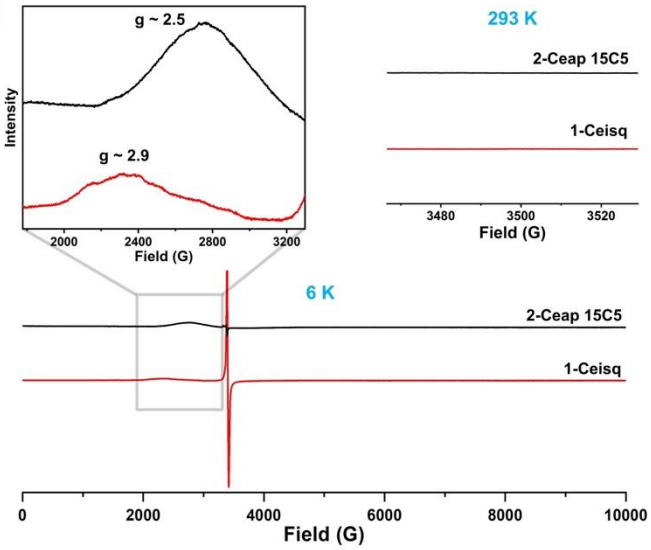

Figure 6: EPR characterization of 10 mM THF solutions of **1-Ceisq** and **2-Ceap 15c5**. EPR spectra recorded at room temperature (293 K, top right). EPR spectra obtained at a low temperature of 6 K (below) with a zoomed view of the spectral alterations.

The oxidation of cerium has been reported previously, and the redox potential varies widely depending on the electrolyte used (1.28 V in 1M HCl to 1.74 V in 1M $HClO_4$ vs. standard hydrogen electrode).[24, 25] ^{1}H NMR spectra of **3-Ceap 15c5** and **3-Ceap crypt** support cerium oxidation, however, as both were both diamagnetic and had resonances for the crypt/crown protons; diamagnetism is expected given that both the amidophenolate ligand and cerium centre (which is now cerium(IV), f^0) are closed shell. The ligand resonances remained non-integrable due to the large crown/crypt peaks similar as for **2-Ceap 15c5** and **2-Ceap crypt** (Figures S6 and S7).

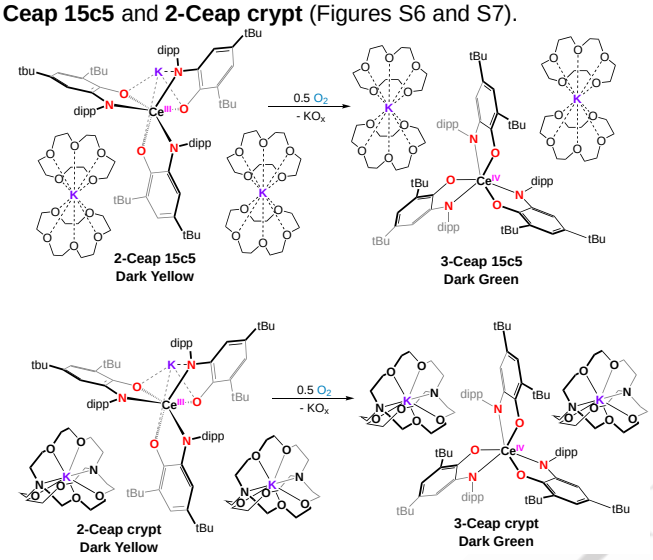

Scheme 3: Synthesis of **3-Ceap 15c5** and **3-Ceap crypt.**

Single crystals for X-ray diffraction for both **3-Ceap 15c5** and **3-Ceap crypt** were grown from a THF: pentane (1:1) solution at ambient temperature. Refinement of the crystal data revealed that both complexes are 6 coordinate with distorted octahedral geometries. Structural parameters showed that C-O and C-N bond lengths similar to **2-Ceap 15c5** (Figures 7 and 8). The C-O bond lengths were 1.313(12)-1.334(11) Å and 1.339(2) Å for **3-Ceap 15c5** and **3-Ceap crypt,** respectively; this is within the range that was observed for **2-Ceap 15c5** at 1.335(2)-1.338(3) Å. The C-N bond lengths were 1.396(12)-1.408(12) Å and 1.390(2) Å for **3-Ceap 15c5** and **3-Ceap crypt** respectively; this is within the range that was observed for **2-Ceap 15c5** at 1.387(3)-1.433(17) Å. The Ce-O and Ce-N bond lengths were shorter for both **3-Ceap 15c5** and **3-Ceap crypt** compared to **2-Ceap 15c5**. This can be rationalized by the fact that the cerium center in both **3-Ceap 15c5** and **3-Ceap crypt** is in the +4 oxidation state while it is in the +3 configuration for **2-Ceap 15c5**; this is consistent with the difference in ionic radii.

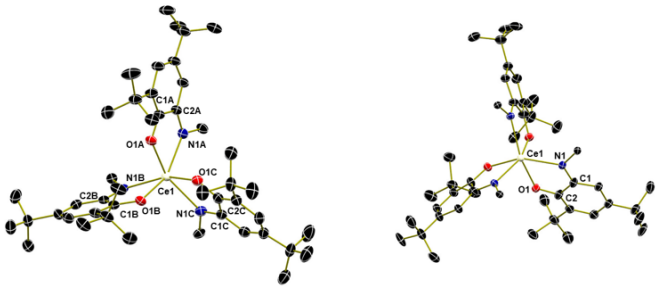

Figure 7: Molecular structures of **3-Ceap 15c5** (left) and **3-Ceap crypt** (right) shown with 30% probability ellipsoids. Hydrogen atoms, dipp groups, sequestered potassium ions with crowns/ crypts, and co-crystallized solvent molecules are omitted for clarity.

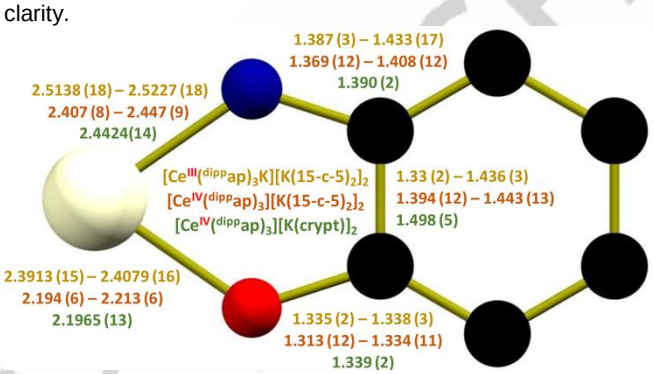

Figure 8. Bond distance comparison (Å) for **2-Ceap 15c5** (gold), **3-Ceap 15c5** (red), and **3-Ceap crypt** (green). Carbon atoms shown in black, nitrogen in blue, oxygen in red, and cerium in white.

As for the trivalent cerium derivatives, the cerium(IV) complex, **3-Ceap 15c5** was also studied using electronic absorption spectroscopy. Collection of a THF solution of **3-Ceap 15c5** at 25 °C shows absorptions in the UV region of the spectrum at 317 nm (ε =27,400 M^{-1} cm^{-1}) and in the visible region at 697 nm (ε = 2190 M^{-1} cm^{-1}) (Figure S12). No absorptions are noted in the NIR region as expected for the Ce(IV), d^0f^0 species.

Cyclic voltammetric data was also collected for the tetravalent cerium derivative, **3-Ceap 15c5**. The features of **3-Ceap 15c5** are similar to that of **2-Ceap 15c5** (Figures S16,17). The Ce(IV/III) couple for **3-Ceap 15c5** is at $E_{1/2}$ = -0.84 V, a shift of ca. 0.16 V negative relative to **2-Ceap 15c5**. This shift could be due to the fact that the Ce(IV) compound does not have an intercalated potassium ion.

To compare the cerium(III) and (IV) compouds, the Ce(4+/3+) couples of all three complexes exhibit quasi-reversible behavior due to the peak current dependence on the square of the scan rate. For **3-Ceap 15c5**, higher scan rates reveal a secondary event at ca. -0.9 V (Figure S16,17). This indicates that a secondary process such as ligand reorganization is involved in the re-oxidation from Ce(III) to Ce(IV) after initial reduction from Ce(IV) to Ce(III). This behavior is not seen in the scan rate variation for **2-Ceap 15c5**, which is evidence of conservation of the potassium ion in the inner sphere.

Addition of excess $Me_3SiOSiMe_3$ to a THF solution of tetravalent **3-Ceap 15c5** resulted in the cleavage of Si-O bonds to form $[(Me_3SiO)_2Ce^{IV}(^{dipp}ap)_2][K(15\text{-}c\text{-}5)_2]_2$ (**4-CeOSiMe$_3$**)

(Scheme 4). Although the mechanism is unclear, the ^{1}H NMR spectrum of washings of the reaction after solvent removal *in vacuo* shows some evidence of free iminoquinone ligand but not hexamethyldisilane (HMDS) (which may be removed *in vacuo*). ^{1}H NMR spectra of 2 equivalents of $Me_3SiOSiMe_3$ added to **3-Ceap 15c5** showed some evidence of a new product appearing in the region where HMDS appears with the consumption of $Me_3SiOSiMe_3$ after 30 minutes (Figure S8). A ^{29}Si NMR spectrum only revealed a single resonance assigned as HMDS (Figure S8). Further NMR studies are necessary to fully confirm the mechanistic pathway.

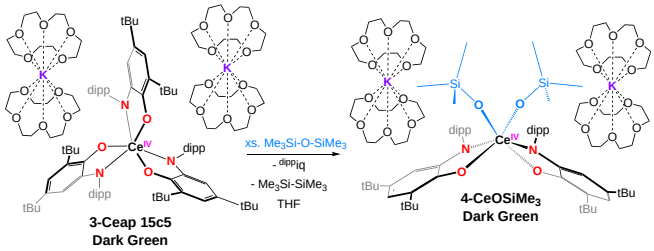

Scheme 4: Synthesis of **4-CeOSiMe$_3$**.

The ^{1}H NMR spectrum of **4-CeOSiMe$_3$** only displayed resonances for the crown and $OSiMe_3$ methyl peaks (Figure S9). Single crystals of **4-CeOSiMe$_3$** for X-ray diffraction were grown from a THF: $Me_3SiOSiMe_3$ (1:1) solution at ambient temperature (Figure S18). Refinement of the data showed six coordinate, distorted octahedral cerium ions. Based on the quality of the solid state structure, the discussion of bond distances must be approached with care. With these data, connectivity is established that shows the two new -$OSiMe_3$ ligands, with the data quality around the cerium ion being sufficient. However, the ligand distances are not accurate for meaningful discussion. The Ce-$OSiMe_3$ bond lengths are 2.167(8) Å and 2.174(6) Å, which are within the range of other published Ce(IV)-$OSiMe_3$ compounds,[26-28] and the Ce-N and C-O bond lengths are within the range of those of **3-Ceap 15c5.** Based on the two -$OSiMe_3$ ligands and the presence of two potassium counterions, the connectivity molecular structure supports the chelating ligands are in the amidophenolate resonance form, both as dianions.

Formation of **4-CeOSiMe$_3$** is significant as it shows a 2-electron oxidation occurred at one of the amidophenolate ligands, generating the iminoquinone. This ligand is labile, and is easily lost during the reaction, thus it is observed by NMR spectroscopy. Alternatively, two different amidophenolate ligands could have been oxidized simultaneously to leave two iminosemiquinone ligands. This tris(ligand) environment may be too sterically crowded with the trimethylsiloxy groups added, and thus extrusion of a neutral ligand was favored over retention of the two 1-electron oxidized ligands.

This observed behavior is divergent from the iodine oxidation to form **1-Ce isq**, and this is consistent with electrochemical data. The ligand-based isq/ap events for **2-Ceap 15c5** and **3-Ceap 15c5** are similar, with two positive and one negative event relative to the Ce(4+/3+) couple (**Figure S_**). The electrochemical behavior of **2-Ceap** differs, with no observed ligand-based event negative couple and multiple events positive relative to the Ce(4+/3+) couple. This shifting of the ligand-based redox events is consequential for the difference in reactivity behavior; the oxidation of **2-Ceap** forms **1-Ceisq**, while the oxidation of **2-Ceap 15c5** forms **3-Ceap 15c5** due to the difference in oxidation potentials of the ligands.

Conclusion

In summary, a family of cerium complexes containing ligands in different oxidation states of the the iminobenzoquinone, 4,6-di-tert-butyl-N-(2,6-di-isopropylphenyl)-o-iminobenzoquinone (^{dipp}iq), was synthesized. Several complexes of the amidophenolate derivative, **2-Ceap**, were synthesized using 18-c-6, 15-c-5, and cryptand: **2-Ceap 18c6, 2-Ceap 15c5,** and **2-Ceap crypt.** A focal point of this work is the oxidation chemistry, as oxidation occurs either at the cerium or at the ligand. An example of the former is the oxidation of trivalent **2-Ceap 15c5** and **2-Ceap crypt** with dioxygen, which results in the oxidation of the cerium(III) to cerium(IV), generating **3-Ceap 15c5 and 3-Ceap crypt**. In the latter case, oxidation of the amidophenolates in **2-Ceap** with elemental iodine forms the tri(iminosemiquinone) compound, **1-Ceisq**, which features three ligand radicals. In general, tri(radical) complexes such as these are rare.[29] Only two lanthanide tri(radical) complexes (with gadolinium and dysprosium) have to our knowledge been isolated and they have been synthesized with nitronyl nitroxide based ligands that contain all three radicals on the same ligand.[30, 31] **1-Ceisq** is the first complex with three separate ligand radicals on a lanthanide centre. Interestingly, addition of hexamethyldisiloxane to a THF solution of **3-Ceap 15c5** resulted in the cleavage of Si-O bonds, furnishing **4-CeOSiMe$_3$.** The identities of all complexes were supported by ^{1}H NMR spectroscopy and crystallography. Future work will focus on the synthesis and characterization of more oxidation products, with a specific eye towards terminal multiply bound ligands.

Experimental Section

General Considerations. All air- and moisture-sensitive manipulations were performed using standard Schlenk techniques or in an MBraun inert atmosphere drybox with an atmosphere of purified nitrogen. The Mbraun drybox was equipped with a cold well designed for freezing samples in liquid nitrogen as well as two −35 °C freezers for cooling samples and crystallizations. Solvents for sensitive manipulations were dried and deoxygenated using literature procedures with a Seca solvent purification system.[32] Benzene-d_6 was purchased from Cambridge Isotope Laboratories, dried with molecular sieves and sodium, and degassed by three freeze−pump−thaw cycles. Pyridine-d_5 was purchased from Cambridge Isotope Laboratories, dried over CaH_2, distilled, degassed by three freeze−pump−thaw cycles, and stored over molecular sieves 24 hours before use. HMDSO was dried over CaH_2, distilled, degassed by three freeze−pump−thaw cycles, and stored over molecular sieves 24 hours before use. 4,6-Di-tert-butyl-2-[(2,6-diisopropylphenyl)-imino]quinone (^{dipp}iq)[33] and potassium graphite (KC_8),[34] prepared according to literature procedures. 15-crown-5 was dried with molecular sieves and degassed by three

freeze−pump−thaw cycles and placed on fresh sieves in the drybox for 24 hours prior to use.[35] Cryptand and cerium trichloride ($CeCl_3$) was dried on the Schlenk line overnight prior to use. Oxygen (≥ 99.6%, ≤10 ppm water) and dry air (≤10 ppm water) cylinders were purchased from Sigma Aldrich and used without further purification.

^{1}H NMR spectra were recorded on a Varian Inova 300 or Bruker AV-III-HD-400 spectrometer operating at 299.99 and 400.13 MHz, respectively. Variable temperature ^{1}H NMR spectra were recorded on a Bruker AV-III-HD-500 spectrometer operating at 500.13 MHz. All chemical shifts were reported relative to the peak for $SiMe_4$ using ^{1}H (residual) chemical shifts of the solvent as a secondary standard. The spectra for paramagnetic molecules were obtained using an acquisition time of 0.5 s; thus, the peak widths reported have an error of ±2 Hz. For paramagnetic molecules, the ^{1}H NMR data are reported with the chemical shift, followed by the peak width at half height in hertz, the integration value, and where possible, the peak assignment. Electronic absorption measurements were recorded at 294 K in THF in sealed, 1 cm quartz cuvettes with a Cary 6000i UV−vis/NIR spectrophotometer. Solid state infrared spectra were recorded using a Thermo Nicolet 6700 spectrophotometer. Samples were made by crushing the solids, mixing with dry KBr, and pressing into a pellet.

All EPR spectra were recorded on a Bruker EMXplus EPR system, integrated with a ColdEdge Stinger closed-cycle flow system for low-temperature measurements. The EPR samples, each containing approximately 10 mM of Ce complexes dissolved in THF, were prepared anaerobically inside a glovebox. Following preparation, they were rapidly frozen and stored in liquid nitrogen. For the detection of Ce(III) signals, the EPR spectra were recorded at 6 K with the following conditions: modulation amplitude 8 G, microwave power 1.0 mW, and microwave frequency ~ 9.5 GHz. To probe the characteristics of organic radicals, room-temperature EPR spectra were recorded with the following conditions: modulation amplitude 0.2 G, microwave power 1.0 mW, and microwave frequency ~ 9.8 GHz.

Electrochemical experiments were carried out using a CHI 620e potentiostat in an inert atmosphere. The electrochemical cell consisted of a glassy carbon working electrode, platinum coil auxiliary electrode, AgCl coated silver wire reference electrode. Each sample consisted of 5 mL THF, 0.1 M tetrabutylammonium hexafluorophosphate (NBu_4PF_6), and 0.5 mM analyte (0.003 g **2-Ceap**, 0.006 g **2-Ceap 15c5**, 0.006 g **3-Ceap 15c5**). Potentials were externally referenced versus 1 mM Ferrocene (0 V) after completion of experiments. Open Circuit Potentials were recorded before each CV scan. Full cyclic voltammograms were recorded between the ends of the solvent window using 100 mV/s scans, 5 second quiet time, and an appropriate amount of iR compensation. The cerium 4+/3+ redox couple was isolated between benign potentials and a series of CVs were collected at 50, 100, 200, 400, 800, and 1600 mV/s scan rates. Estimated standard deviation for redox couples are ± 50 mV.

Synthesis of $Ce^{III}(^{dipp}isq)_3$ (1-Ceisq). A 20 mL scintillation vial was charged with $CeCl_3$ (0.150 g, 0.609 mmol) and 3 mL THF. A separate 20 mL scintillation vial was charged with ^{dipp}iq (0.693 g, 1.8257 mmol), dissolved in 3 mL THF, and added dropwise to the stirring $CeCl_3$ slurry. Potassium graphite (0.171 g, 1.26 mmol) was added slowly (~30 mg every 45 seconds), resulting in a rapid color change from red-brown to dark green. After 2 hours, the solution was filtered over a celite pad and volatiles were removed in vacuo. A dark green powder was isolated (with impurities) and assigned as $Ce^{III}(^{dipp}isq)_3$ *(***1-Ceisq***)*. Crystals suitable for X-ray analysis were obtained from evaporation of a concentrated hexane at room temperature. ^{1}H NMR (C_6D_6, 300 MHz, 25 °C): δ = 2.88, 1.73, 13.19, 14.64, 15.64, 16.21, 16.38, 30.94, 38.89, 46.94. Calcd For $C_{78}H_{111}N_3O_3Ce$: C, 73.26; H 8.75; N, 3.28. Found C, 72.94; H, 8.91; N, 3.21.

Synthesis of $Ce^{III}(^{dipp}isq)_3$ (1-Ceisq) from 2-Ceap*.* A 20 mL scintillation vial was charged with **2-Ceap** (0.100 g, 0.0716 mmol) and 3 mL THF. A separate 20 mL scintillation vial was charged with I_2 (18 mg, 0.107 mmol) and dissolved in 3 mL THF. The I_2 solution was added dropwise to the **2-Ceap** solution and stirred overnight. The mixture was filtered over a Celite frit to remove KI and volatiles were removed in vacuo. A crude dark green product (contains further oxidized ligand) was obtained and was concluded to be **1-Ceisq** (0.085 g, 0.0665 mmol, 92% yield) based on ^{1}H NMR.

Synthesis of $[Ce^{III}(^{dipp}ap)_3K][K(15\text{-}c\text{-}5)_2]_2$ (2-Ceap 15c5). A 20 mL scintillation vial was charged with **2-Ceap** (0.250 g, 0.179 mmol) and 3 mL THF. 4.1 equivalents of 15-crown-5 (0.162 g, 0.734 mmol) was added dropwise to the stirring **2-Ceap** solution. Darkening of the solution was observed. After 1 hour, volatiles were removed in vacuo. The crude mixture was washed with diethyl ether (2 x 5 mL) and dried in vacuo to afford a golden yellow powder (0.358 g, 0.152 mmol, 85% yield), assigned as **$[Ce^{III}(^{dipp}ap)_3K][K(15\text{-}c\text{-}5)_2]_2$** (**2-Ceap 15c5**). Yellow, needle-shaped crystals suitable for X-ray analysis were grown overnight from a THF solution layered with pentane (1:1) at -35°C. ^{1}H NMR (pyr-d5, 300 MHz, 25 °C): δ = -13.48, 1.98, 1.17, 1.45, 1.56, 2.00, 3.50 (s, 80H, 15-c-5), 6.09, 6.49, 7.32, 9.07, 9.49, 12.58. *Note that ligand peaks cannot be conclusively assigned or integrated due to the large intensity of the 15-C-5 peak overwhelming the ligand peaks.* Calcd For $C_{118}H_{191}N_3O_{23}K_3Ce$: C, 62.24; H 8.45; N, 1.85. Found C, 61.44; H, 8.26; N, 1.96.

Synthesis of $[Ce^{III}(^{dipp}ap)_3K][K(crypt)]_2$ (2-Ceap crypt). A 20 mL scintillation vial was charged with **2-Ceap** (0.250 g, 0.179 mmol) and a 3 mL THF solution of 2.1 equivalents of cryptand (0.143 g, 0.377 mmol) was added dropwise to the stirring **2-Ceap** solution. Darkening of the solution was observed. After 1 hour, volatiles were removed in vacuo. The crude mixture was washed with diethyl ether (2 x 5 mL) and dried in vacuo to afford a golden yellow powder (0.351 g, 0.163 mmol, 91% yield), assigned as **$[Ce^{III}(^{dipp}ap)_3K][K(crypt)]_2$** (**2-Ceap crypt**). ^{1}H NMR (pyr-d_5, 300 MHz, 25 °C): δ = -13.53, -11.37, -3.05, -1.99, -1.70, 1.23, 1.50, 2.15, 2.34, 3.35, 3.40, 3.75, 4.11, 4.59, 11.74, 13.22, 15.87. *Note that ligand peaks cannot be conclusively assigned or integrated due to the large intensity of the cryptand peaks overwhelming the ligand peaks.* $C_{114}H_{183}N_7O_{15}K_3Ce$: C, 63.71; H 8.58; N, 4.56. Found C, 62.00; H, 8.29; N, 4.70. These results are consistent with incomplete combustion of the sample.

Synthesis of $[Ce^{IV}(^{dipp}ap)_3][K(15\text{-}c\text{-}5)_2]_2$ (3-Ceap 15c5). A 100 mL side-arm Schlenk bomb flask with a Teflon stopcock was charged with **2-Ceap 15c5** (0.500 g, 0.213 mmol) and 10 mL of THF in a glovebox and sealed. Outside the glovebox, the flask was connected to a 37.1 mL calibrated glass bulb with Teflon stopcocks which in turn was connected to a high-vacuum Schlenk line and evacuated. The **2-Ceap 15c5** solution was frozen in the flask with a liquid N_2 bath and the remaining space in the bomb was evacuated. Assuming ideal gas behavior, the glass bulb was filled with O_2 to a pressure of 56 mm Hg via the Schlenk line using a brass control valve attached to a metal cylinder charged with O_2.

The O_2 gas trapped in the glass bulb was then condensed into the flask containing **2-Ceap 15c5** (about 5 min). The flask was sealed and the liquid N_2 bath was removed, and the reaction was stirred while allowing it to reach room temperature. Immediately after thawing, a green solution was observed. After stirring overnight, the volatiles were removed in vacuo on the high-vacuum line and bought into the glovebox. The resulting green solid was washed with pentane (3 x 5 mL). Volatiles were removed in vacuo to afford a green powder (0.472 g, 0.204 mmol, 96% yield), assigned as $[Ce^{IV}(^{dipp}ap)_3][K(15\text{-}c\text{-}5)_2]_2$ (**3-Ceap 15c5**). Yellow-green, needle-shaped crystals suitable for X-ray analysis were grown overnight from a THF solution layered with pentane (1:1 ratio) in a narrow, sealed J-young tube at room temperature. ^{1}H NMR (pyr-d5, 300 MHz, 25 °C): δ = 1.23, 1.35, 1.44, 1.68, 2.01, 2.29, 3.54 (s, 80H, 15-c-5), 5.13, 5.63, 6.38, 6.49, 7.30, 7.49. *Note that ligand peaks cannot be conclusively assigned or integrated due to the large intensity of the 15-C-5 peak overwhelming the ligand peaks.* Calcd For $C_{118}H_{191}N_3O_{23}K_2Ce$: C, 63.32; H 8.60; N, 1.88. Found C, 61.58; H, 8.34; N, 1.96. These results are consistent with incomplete combustion.

Synthesis of $[Ce^{IV}(^{dipp}ap)_3][K(crypt)]_2$ (3-Ceap crypt). A 100 mL side-arm Schlenk bomb flask with a Teflon stopcock was charged with **2-Ceap crypt** (0.250 g, 0.116 mmol) and 10 mL of THF in a glovebox and sealed. Outside the glovebox, the flask was connected to a 37.1 mL calibrated glass bulb with Teflon stopcocks which in turn was connected to a high-vacuum Schlenk line and evacuated. The **2-Ceap crypt** solution was frozen in the flask with a liquid N_2 bath and the remaining space in the bomb was evacuated. Assuming ideal gas behavior, the glass bulb was filled with O_2 to a pressure of 31 mm Hg via the Schlenk line using a brass control valve attached to a metal cylinder charged with O_2. The O_2 gas trapped in the glass bulb was then condensed into the flask containing **2-Ceap crypt** (about 5 min). The flask was sealed and the liquid N_2 bath was removed, and the reaction was stirred while allowing it to reach room temperature. Immediately after thawing, a green solution was observed. After stirring overnight, the volatiles were removed in vacuo on the high-vacuum line and bought into the glovebox. The resulting green solid was washed with pentane (3 x 5 mL). Volatiles were removed in vacuo to afford a green powder assigned as $[Ce^{IV}(^{dipp}ap)_3][K(15\text{-}c\text{-}5)_2]_2$ (**3-Ceap crypt**). Yellow, needle-shaped crystals suitable for X-ray analysis were grown overnight from a THF solution layered with pentane (1:1 ratio) in a narrow, sealed J-young tube at room temperature. ^{1}H NMR (pyr-d5, 300 MHz, 25 °C): δ = 1.23, 1.49, 1.66, 1.99, 2.13, 2.40, 3.39, 3.44, 3.86, 6.58, 7.16, 7.30, 8.43. *Note that ligand peaks cannot be conclusively assigned or integrated due to the large intensity of the cryptand peaks overwhelming the ligand peaks.* Calcd For $C_{114}H_{183}N_7O_{15}K_2Ce$: C, 64.89; H 8.74; N, 4.65. Found C, 61.57; H, 8.31; N, 4.43. These results are consistent with incomplete combustion.

Synthesis of $[(Me_3SiO)_2Ce^{IV}(^{dipp}ap)_2][K(15\text{-}c\text{-}5)_2]_2$ (4-CeOSiMe$_3$). A 20 mL scintillation vial was charged with **3-Ceap 15c5** (0.050 g, 0.0447 mmol), 3 mL THF, and 5 mL HMDSO (excess). The reaction mixture was stirred overnight, and volatiles removed under vacuo. The resulting green solid was washed with pentane (5 x 5 mL). Volatiles were removed in vacuo to afford a green powder (0.036 g. 0.017 mmol, 79% yield) assigned as $[(Me_3SiO)_2Ce^{IV}(^{dipp}ap)_2][K(15\text{-}c\text{-}5)_2]_2$ (**4-CeOSiMe$_3$**). ^{1}H NMR (C_6D_6, 300 MHz, 25 °C): δ = 1.55 ($OSiMe_3$), 3.22 (15-c-5). $C_{98}H_{172}N_2O_{24}Si_2K_2Ce$: C, 57.79; H 8.51; N, 1.38. Found C, 58.64; H, 8.07; N, 1.81.

Supporting Information

The authors have cited additional references within the Supporting Information. The following files are available free of charge: NMR, UV-vis/NIR, FT-IR, crystallographic data and refinement parameters.

Acknowledgements

This material is based upon work supported by the U.S. Department of Energy, Office of Science, Office of Basic Energy Sciences, Heavy Element Chemistry Program under Award Number DE-SC0008479. A.W.M. acknowledges the National Science Foundation for support under the Graduate Research Fellowship Program (GRFP) under grant number DGE-1842166 (electronic absorption spectroscopy and elemental analysis).

Conflicts of Interest

The authors declare no competing financial interest.

Data Availability Statement

The data that support the findings of this study are available on request from the corresponding author. These data are not publicly available due to privacy or ethical restrictions.

Keywords: cerium • redox-active ligands • ligand radicals • oxidation

[1] N. Kaltsoyannis, P. Scott, *The f elements*, Oxford University Press, New York, **1999**.
[2] N. T. Rice, J. Su, T. P. Gompa, D. R. Russo, J. Telser, L. Palatinus, J. Bacsa, P. Yang, E. R. Batista, H. S. La Pierre, *Inorg. Chem.* **2019**, *58*, 5289-5304.
[3] P. B. Hitchcock, M. F. Lappert, A. V. Protchenko, *Chemical Communications* **2006**, 3546-3548.
[4] Y. Wang, J. Liang, C. Deng, R. Sun, P.-X. Fu, B.-W. Wang, S. Gao, W. Huang, *J. Am. Chem. Soc.* **2023**, *145*, 22466-22474.
[5] K. J. Blackmore, J. W. Ziller, A. F. Heyduk, *Inorg. Chem.* **2005**, *44*, 5559-5561.
[6] E. J. Coughlin, Y. Qiao, E. Lapsheva, M. Zeller, E. J. Schelter, S. C. Bart, *J. Am. Chem. Soc.* **2019**, *141*, 1016-1026.
[7] E. J. Coughlin, M. Zeller, S. C. Bart, *Angew. Chem., Int. Ed.* **2017**, *56*, 12142-12145.
[8] M. E. Garner, J. Arnold, *Organometallics* **2017**, *36*, 4511-4514.
[9] I. L. Fedushkin, O. V. Maslova, A. G. Morozov, S. Dechert, S. Demeshko, F. Meyer, *Angew. Chem., Int. Ed.* **2012**, *51*, 10584-10587.
[10] I. L. Fedushkin, O. V. Maslova, A. N. Lukoyanov, G. K. Fukin, *C. R. Chim.* **2010**, *13*, 584-592.
[11] I. L. Fedushkin, O. V. Maslova, E. V. Baranov, A. S. Shavyrin, *Inorg. Chem.* **2009**, *48*, 2355-2357.
[12] H. Schumann, M. Hummert, A. N. Lukoyanov, V. A. Chudakova, I. L. Fedushkin, *Z. Naturforsch., B: Chem. Sci.* **2007**, *62*, 1107-1111.
[13] V. A. Dodonov, V. M. Makarov, M. N. Zemnyukova, D. A. Razborov, E. V. Baranov, A. S. Bogomyakov, V. I. Ovcharenko, I. L. Fedushkin, *Organometallics* **2023**, *42*, 2558-2567.

[14] F.-C. Hsueh, T. Rajeshkumar, L. Maron, R. Scopelliti, A. Sienkiewicz, M. Mazzanti, *Chemical Science* **2023**, *14*, 6011-6021.
[15] D. M. R. Y. P. Rupasinghe, H. Gupta, M. R. Baxter, R. F. Higgins, M. Zeller, E. J. Schelter, S. C. Bart, *Inorg. Chem.* **2021**, *60*, 14302-14309.
[16] D. M. R. Y. P. Rupasinghe, M. R. Baxter, H. Gupta, A. T. Poore, R. F. Higgins, M. Zeller, S. Tian, E. J. Schelter, S. C. Bart, *J. Am. Chem. Soc.* **2022**, *144*, 17423-17431.
[17] C. Uruburo, D. M. R. Y. P. Rupasinghe, H. Gupta, R. M. Knieser, L. M. Lopez, M. H. Furigay, R. F. Higgins, P. Pandey, M. R. Baxter, P. J. Carroll, M. Zeller, S. C. Bart, E. J. Schelter, *Inorg. Chem.* **2023**.
[18] G. W. Gokel, in *Crown Ethers and Cryptands*, The Royal Society of Chemistry, **1991**, pp. 64-98.
[19] W. Zhu, X. Wu, C. He, C. Duan, *Tetrahedron* **2013**, *69*, 10477-10481.
[20] E. Iravani, N. Nami, F. Nabizadeh, E. Bayani, B. Neumuller, *Bull. Korean Chem. Soc* **2013**, *34*, 3420-3424.
[21] D. Schneider, T. Spallek, C. Maichle-Mössmer, K. W. Törnroos, R. Anwander, *Chem. Commun.* **2014**, *50*, 14763-14766.
[22] M. Ghose, S. Banerjee, S. Patra, K. K. Mukherjea, *J. Lumin.* **2016**, *180*, 224-233.
[23] A. B. Abragam, B. , *Electron Paramagnetic Resonance of Transition Ions*, Oxford University Press, **1970**.
[24] N. A. Piro, J. R. Robinson, P. J. Walsh, E. J. Schelter, *Coord. Chem. Rev.* **2014**, *260*, 21-36.
[25] S. J. Park, M. H. Joo, J. H. Yang, S.-M. Hong, C. K. Rhee, J.-G. Kang, Y. Sohn, *ACS Appl. Mater. Interfaces* **2021**, *13*, 27594-27611.
[26] L. A. Solola, A. V. Zabula, W. L. Dorfner, B. C. Manor, P. J. Carroll, E. J. Schelter, *J. Am. Chem. Soc.* **2017**, *139*, 2435-2442.
[27] F. Sinclair, J. A. Hlina, J. A. L. Wells, M. P. Shaver, P. L. Arnold, *Dalton Trans.* **2017**, *46*, 10786-10790.
[28] M. K. Assefa, G. Wu, T. W. Hayton, *Chem. Sci.* **2017**, *8*, 7873-7878.
[29] S. Demir, I.-R. Jeon, J. R. Long, T. D. Harris, *Coord. Chem. Rev.* **2015**, *289-290*, 149-176.
[30] Z.-X. Xiao, H. Miao, D. Shao, H.-Y. Wei, Y.-Q. Zhang, X.-Y. Wang, *Chem. Commun.* **2018**, *54*, 9726-9729.
[31] T. Kanetomo, Y. Naoi, M. Enomoto, *Eur. J. Inorg. Chem.* **2021**, *2021*, 1130-1136.
[32] A. B. Pangborn, M. A. Giardello, R. H. Grubbs, R. K. Rosen, F. J. Timmers, *Organometallics* **1996**, *15*, 1518-1520.
[33] G. A. Abakumov, V. K. Cherkasov, A. V. Piskunov, I. N. Meshcheryakova, A. V. Maleeva, A. I. Poddel'skii, G. K. Fukin, *Dokl. Chem.* **2009**, *427*, 168-171.
[34] S. Chakraborty, J. Chattopadhyay, W. Guo, W. E. Billups, *Angew. Chem. Int. Ed.* **2007**, *46*, 4486-4488.
[35] W. L. F. Armarego, D. D. Perrin, *Purification of Laboratory Chemicals, Vol. 4*, **2000**.
[36] Deposition Number(s) <urlhref="https://www.ccdc.cam.ac.uk/services/structures?id=doi:10.1002/###.20220XXX"> 2312520 (for 1-Ceisq), 2312521 (for 2-Ceap 15c5), 2312985 (for 3-Ceap Crypt), 2312986 (for 3-Ceap 15c5) and 2312987 (for 4-CeOSiMe3) </url> contain(s) the supplementary crystallographic data for this paper. These data are provided free of charge by the joint Cambridge Crystallographic Data Centre and Fachinformationszentrum Karlsruhe <urlhref="http://www.ccdc.cam.ac.uk/structures">Access Structures service</url>.

Entry for the Table of Contents

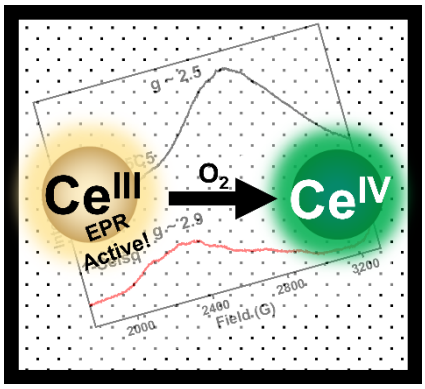

Cerium(III) complexes with redox-active ligands in oxidation states L^{1-} and L^{2-} have been synthesized and fully characterized. Multielectron movement has been achieved by redox chemistry at the ligands. Sequestering counterions also introduces exciting reactivity, forming Ce(IV) species with dioxygen and oxidative addition of hexamethyldisiloxane to form a bis(siloxide) cerium(IV) species.

Twitter username: @TheBartLab